Joint ICTP-IAEA Workshop on Advanced Synchrotron Radiation Based X-ray Spectrometry Techniques, Trieste 2013

Synchrotron Radiation based X-Ray Spectrometry for nanoscaled materials

Matthias Müller, Rainer Unterumsberger, Beatrix Pollakowski and Burkhard Beckhoff

Physikalisch-Technische Bundesanstalt, Berlin

X-Ray and IR- Spectrometry Group

PTB

Outline

- analytical challenges for nanotechnology – a motivation
- reference-free x-ray spectrometry based on synchrotron radiation
- grazing incidence x-ray fluorescence analysis
- calibration standards for sub-monolayer surface contaminations
- nanolayer analysis
- depth profiling and chemical speciation

Challenges for nanotechnologies

Nanoscaled reference materials may be required when

- *critical dimensions* (CD) of specimens and / or
- the analytical *information depths* are in the 1 nm to 100 nm range.

Applications:

- (buried) nanolayered systems to be analyzed by GIXRF or XRF
- low energy ion implantations in silicon or advanced materials by GIXRF
- analysis of nanoscaled objects (Nanoparticles, CNTs, etc.) by GIXRF
- lateral resolution of XRF reaching 100 nm at 3rd generation SR facilities

... and below 1 nm CD:

- analysis of surface contamination (< 0.4 nm) by TXRF
- analysis of buried interfaces and contamination by GIXRF

www.ptb.de/cms/en/fachabteilungen/abt7/fb-72/ag-724.html

Quantitative x-ray fluorescence analysis

Typical XRF quantification variants

α - coefficients

- empirical coefficients
- interpolation regime for main matrix elements or traces in constant matrices
- restricted extrapolation

reference material based

- pre-calibration of instrumentation e.g. by thin standards
- additional calibration by reference materials for specific *applications*
- flexible interpolation by knowledge on FP data

reference-free methodology

- knowledge on both instrumental and fundamental parameters
- increasing relevance for complex sample systems, e.g. nano-scaled specimens
- reason: lack of appropriate reference materials and calibration standards

→ *Less or even no reference materials required*

Analytical challenges for nanoelectronics

Example: nanolayerd materials for semiconductor devices

- X-Ray Fluorescence analysis (XRF) for semiconductors:
  - ✓ non-destructive and non-preparative
  - ✓ fast qualitative results
  - ✓ high sensitivity (ppm), sub-monolayers (fg/cm2)
  - ✓ quantitative results (based on reference materials)
- Semiconductor substrates of interest: Si, Ge, GaAs, InGaAs, InP, InAlAs, etc.
- Hundreds of combinations for nanoscaled thin films
- Lack of appropriate reference materials for nanoscaled systems

Analytical challenges for nanotechnologies

- dozens of new nanoscaled materials appear every month
- technology R&D cycles for new materials down to 4 months
- need for correlation of material properties with functionality
- requirements on sensitivity, selectivity and information depth
- most analytical methodologies rely on reference materials or calibration standards but there are only few at the nanoscale
- usage of calibrated instrumentation and knowledge on atomic data enables reference-free techniques such as SR based XRS

FP-based XRF quantification

Sherman equation for K fluorescence

$$I_{i,j} = I_0(E_k)\,\varepsilon_{eff}(E_{i,j})\,\frac{d\Omega}{4\pi}\cdot e^{-\mu_s(E_k)\rho x/\cos(\Psi_1)}$$

absorption

$$\cdot W_i\,\frac{r_i - 1}{r_i}\,\tau_i(E_k)\,\omega_i\,T_{i,j}\,\frac{1}{\cos(\Psi_1)}\,\Delta x$$

fluorescence production

$$\cdot e^{-\mu_s(E_{i,j})\rho x/\cos(\Psi_2)}$$

absorption

instrumental parameters:
$\varepsilon_{eff}(E_{i,j})$, $d\Omega/4\pi$

atomic fundamental parameters:
μ_s, r_i, τ, ω_i, T_i, ρ

specimen composition
W_i weight fraction of element *i*

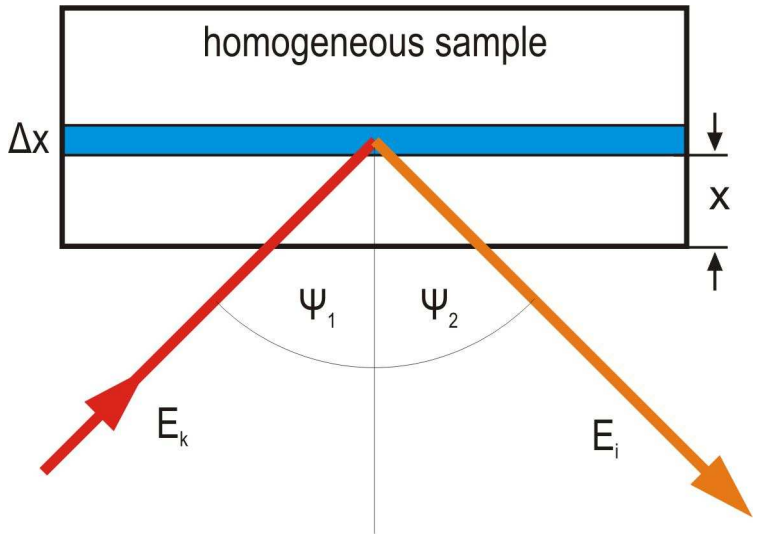

Reference-free X-Ray Fluorescence Analysis

(T)XRF excitation channel

well-known spectral distribution

and radiant power

PTB resources:

→ characterized beamlines

→ calibrated photo diodes

→ calibrated apertures

→ calibrated energy-dispersive detectors

(T)XRF detection channel

absolute detection efficiency

and response behavior

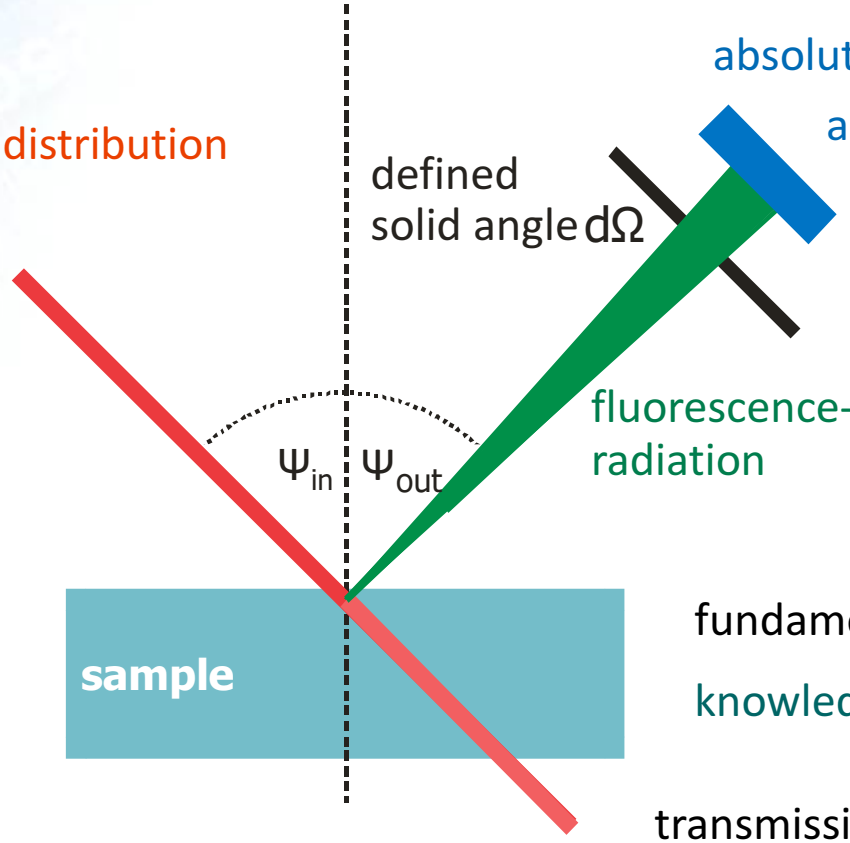

fundamental parameters

knowledge of all parameters

transmission measurements

absorption correction factors

J. Anal. At. Spectrom. ***23****, 845 (2008)*

XRF employing calibrated instrumentation

- 45°/45° geometry: aperture – solid angle of detection
- synchr. rad.: high spectral purity -> low background in XRF and NEXAFS spectra
- incident photon flux: calibrated photo diode - spectral responsivity
- fluorescence radiation: calibrated energy-dispersive detectors, e.g. Si(Li) or SDD

  -> accurate spectral deconvolution and detector efficiency

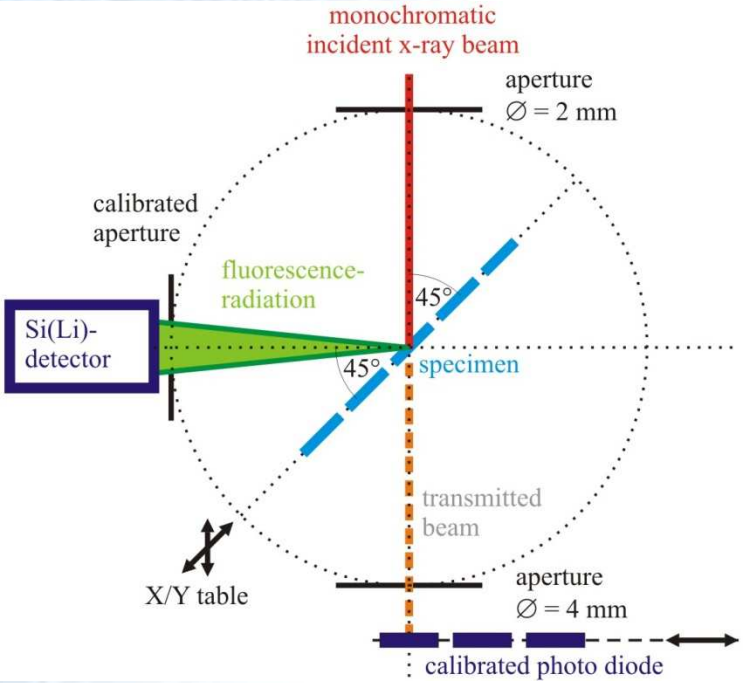

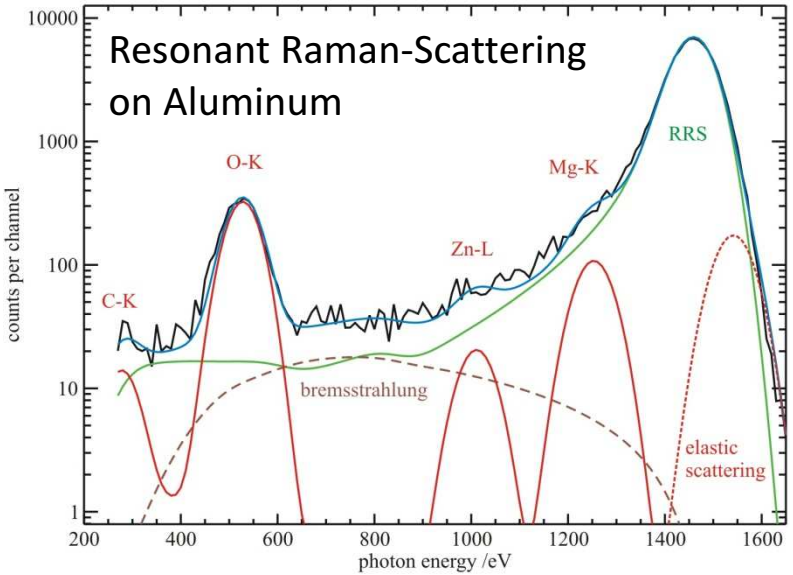

spectral deconvolution XRF spectrum

Grazing incidence geometry (TXRF, GI-XRF)

- grazing incidence -> high sensitivity at surface, nanolayers and interfaces
- characterized beam profile allows for solid angle determination
- calibrated instrumentation -> reference-free GI-XRF measurements
- X-ray Standing Wave (XSW) field have to be taken into account!

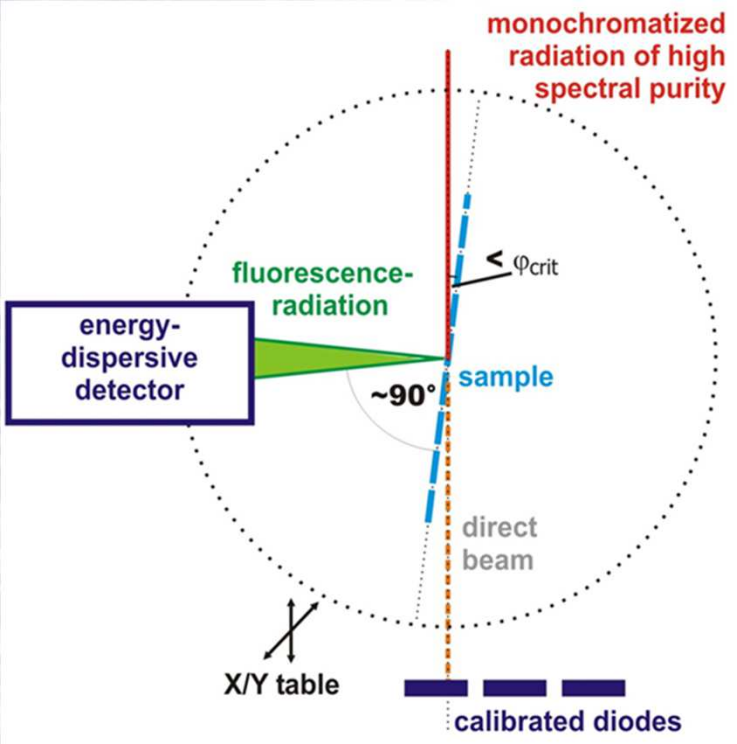

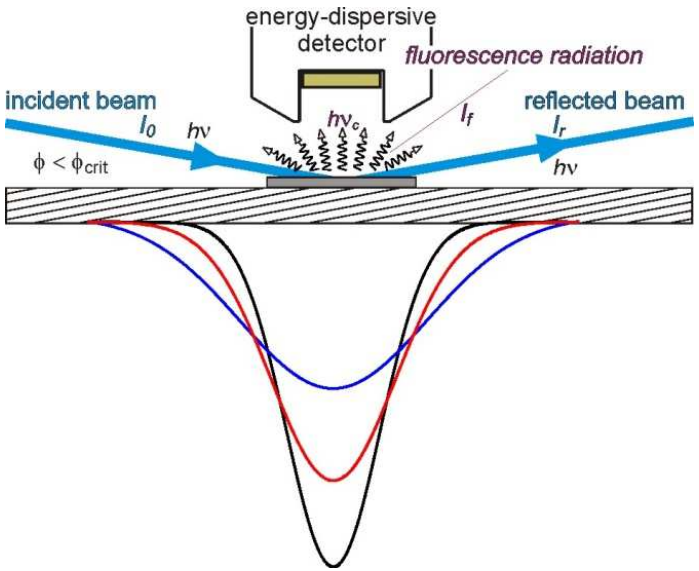

lateral intensity profile effective solid angle of detection

Anal. Chem. 79, 7873−7882 (2007)

Grazing Incidence geometry (TXRF, GI-XRF)

X-ray standing wave field

- constructive interference of incident and reflected beam
- varying intensity with depth can be used for depth profiling
- accurate knowledge needed for reliable quantification

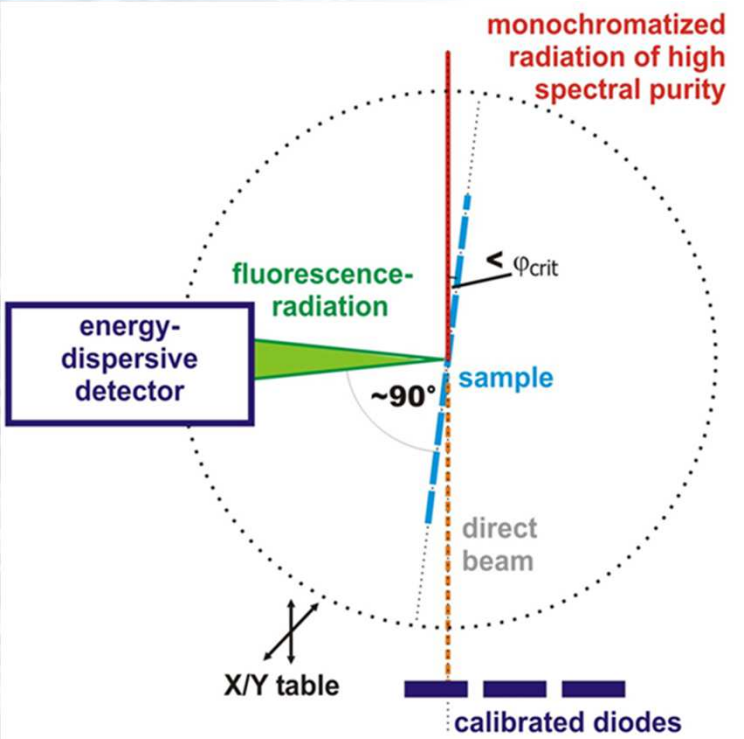

Position (depth) of interference fringes depends on the angle of incidence

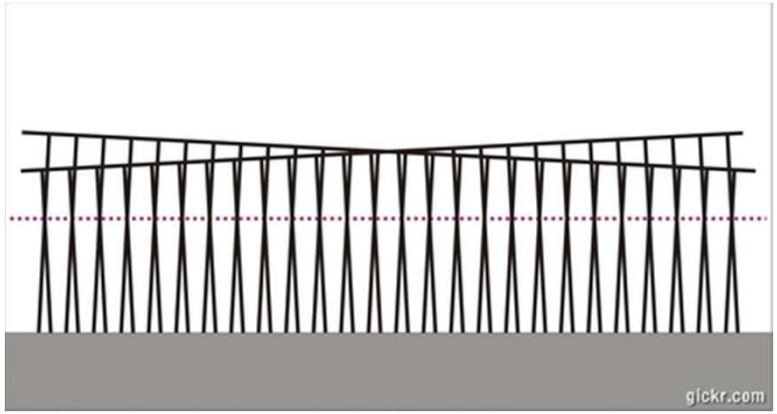

X-ray standing wave field (TXRF, GI-XRF)

- calculation of the XSW field -> free codes available (e.g. IMD*)
- XSW depends on the sample system; e.g. composition, layer thickness, etc.
- iterative XSW calculations for optimization of the sample composition

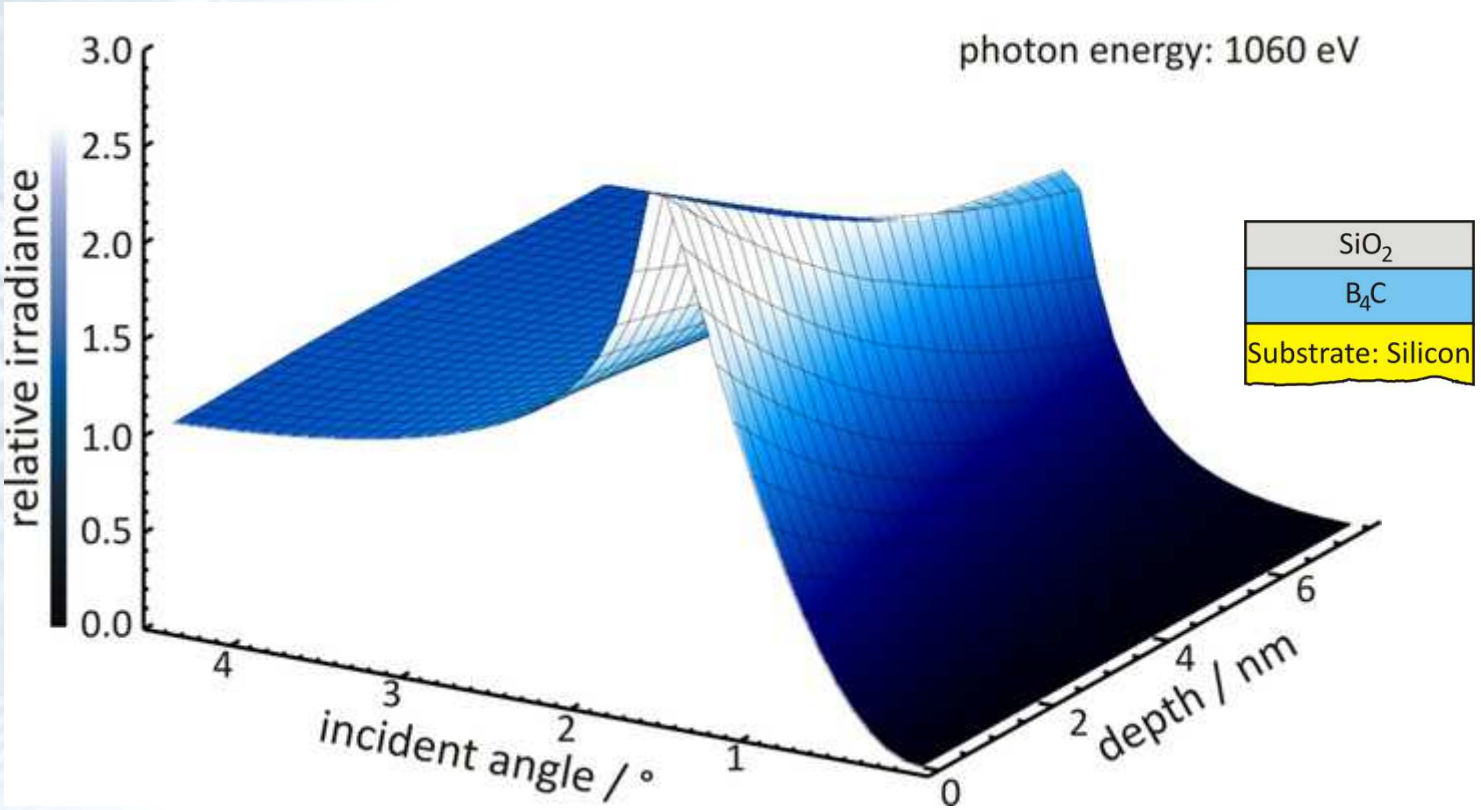

*D.L. Windt, Computers in Physics **12,** 360 (1998)

Outline

- analytical challenges for nanotechnology – a motivation
- reference-free x-ray spectrometry based on synchrotron radiation
- grazing incidence x-ray fluorescence analysis
- calibration standards for sub-monolayer surface contaminations
- nanolayer analysis
- depth profiling and chemical speciation

TXRF for surface analysis

Comparison of various analytical laboratories

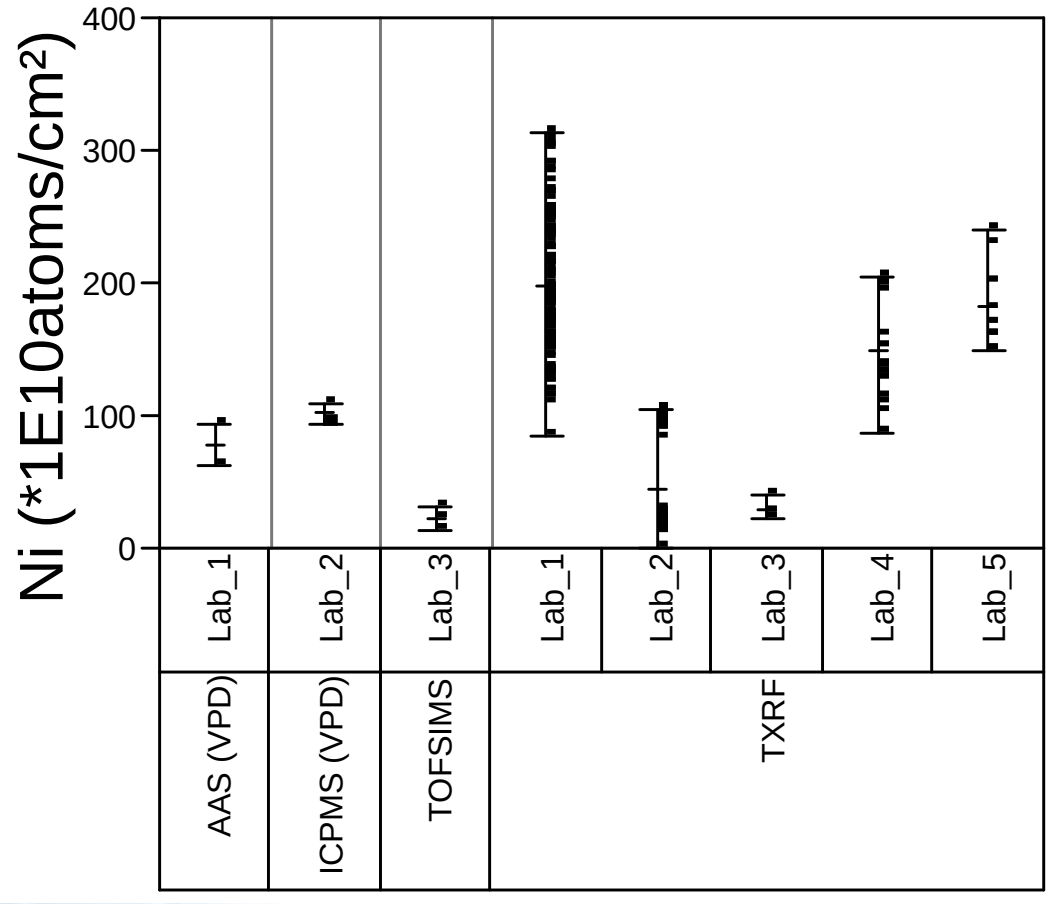

Range of analytical results at various installations

Quantitative analysis of nickel surface contamination on 300 mm silicon wafers.

Controlled contamination by spin-coating, nominal level 10^{12} at/cm^2.

NB: The numbering of the labs and of the analytical methods is not correlated.

Calibration of TXRF

Impact of droplet quality on quantification

Sample information

- 150 mm wafer
- droplets 10, 50, 100, 500, 1000 pg of Mn, Fe, Co, Zn, Ni and Zn

Optical Microscopy

- droplet size scales with Ni amount
- crystallization observed

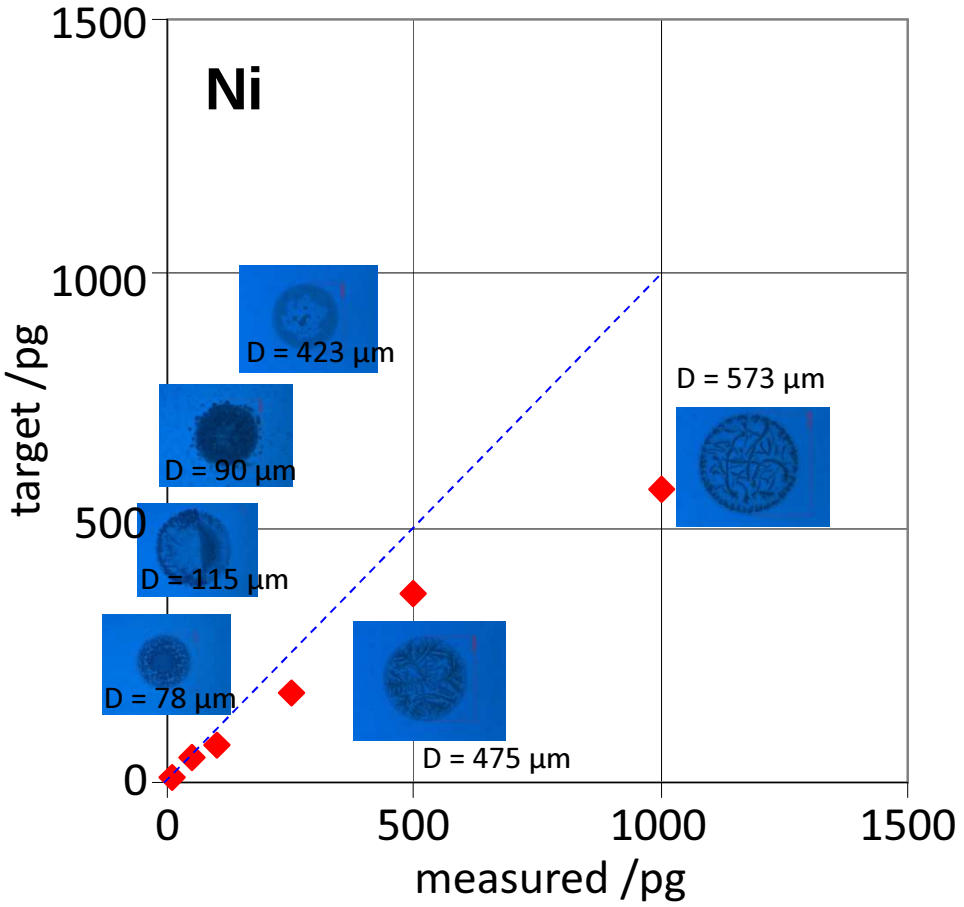

Courtesy of Andreas Nutsch (form. IISB Erlangen)

Analysis by synchrotron radiation based TXRF

Characterization of calibration droplets using a small beam profile

- inhomogeneities and absorption saturation associated with calibration droplets in TXRF analysis
- different shapes of the angular scans

lateral scans

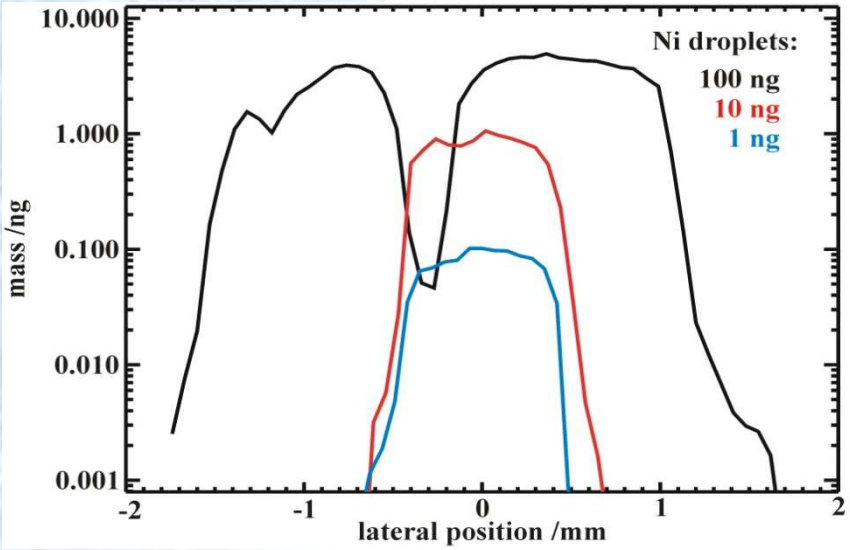

angular scans

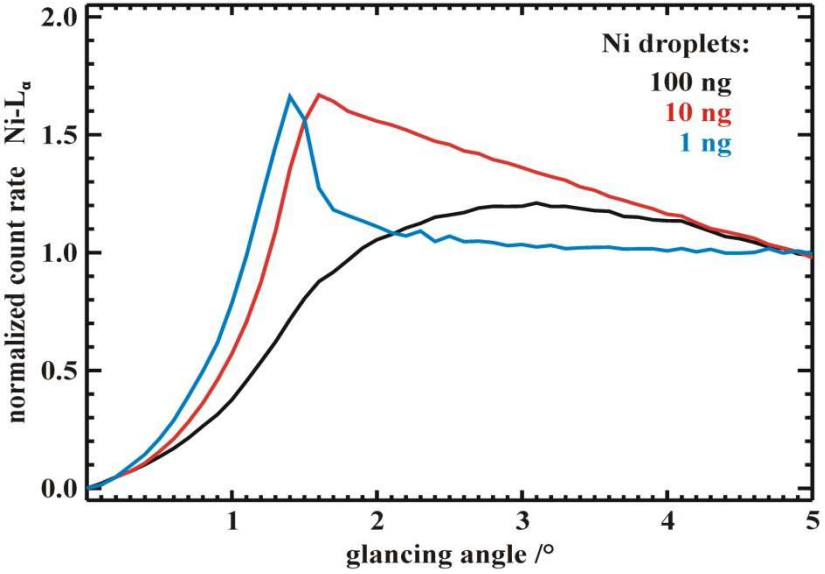

Analysis by synchrotron radiation based TXRF

Characterization of calibration droplets using a small beam profile

Potential reason for deviations in results of pre-calibrated TXRF instruments

Solution: reference-free validation by “lateral slicing” and “angular scanning”

of droplets possible determination of correction factors

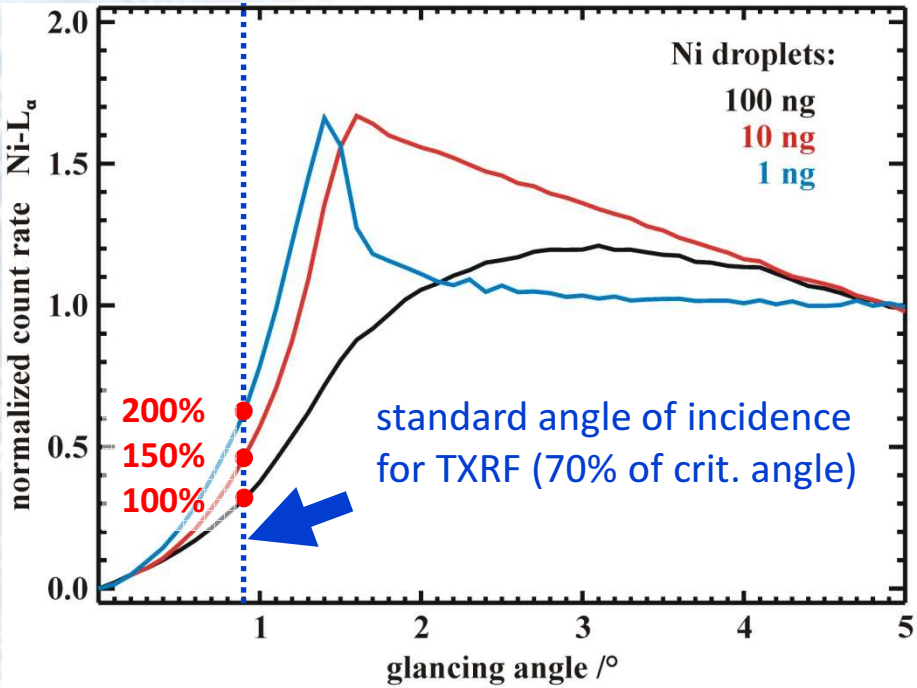

angular scans

Solide State Phenom. 187, p291 (2012)

Reference-free analysis of a calibration droplet

- 1 ng Ni droplet (nominal)
- radiometrically calibrated instrumentation

  (PTB laboratory)
- scanning mass deposition profile with 70 µm beam

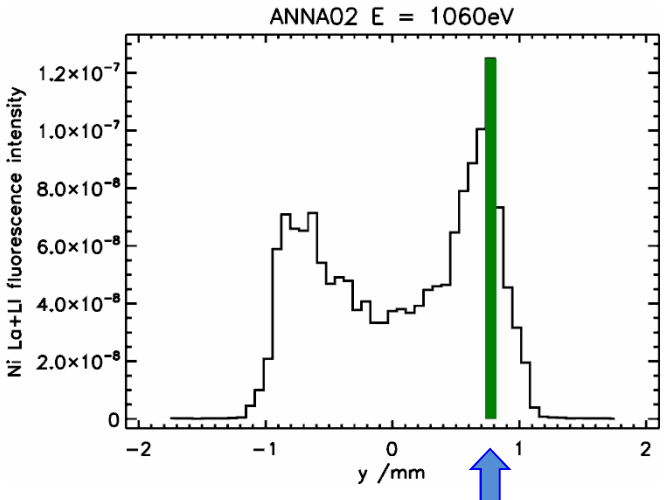

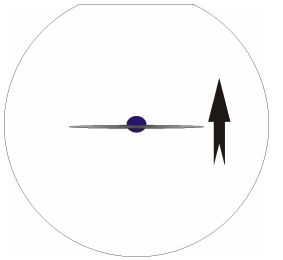

horizontal profile

- mass in beam 69 pg ± 14 pg

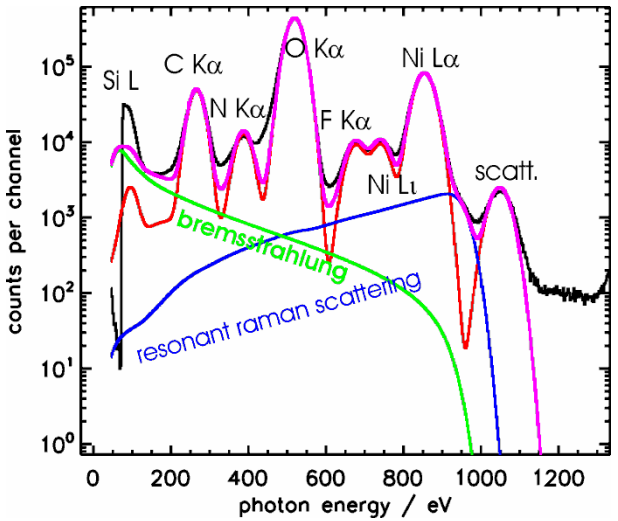

- total droplet mass **890 pg** ± 180 pg

Nanolayer Analysis

Quantification: conventional XRF vs GI-XRF

- nanolayered system, with and without buried metal layer
- the metal layer increases the XSW intensities in the B_4C layer
- Objectives:
  - ➢ determination of the boron carbide layer thickness
  - ➢ validation of the XSW calculations

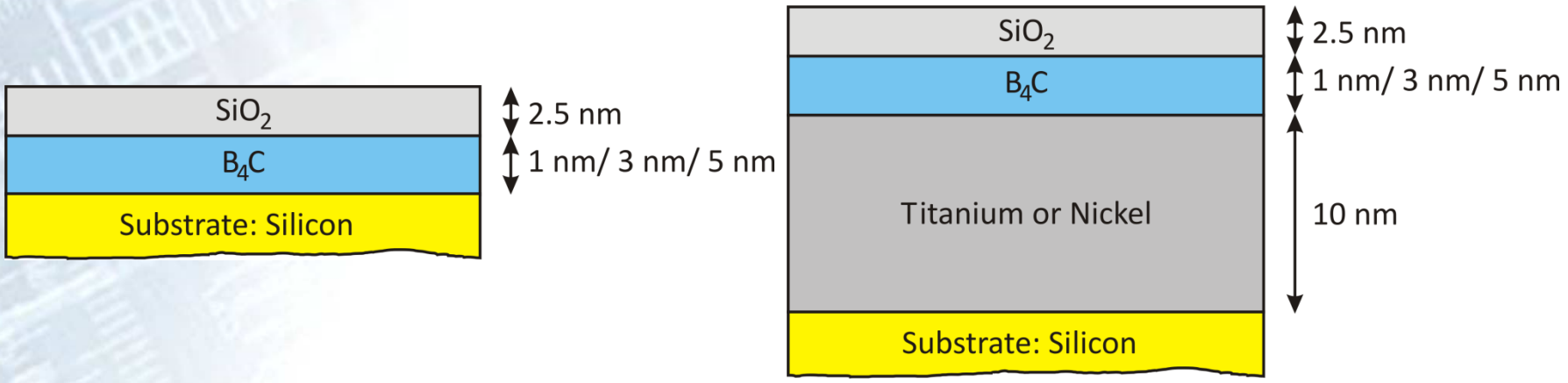

Anal. Chem. 83, 8623-8 (2011)

XRF vs GI-XRF

- UHV chamber allows for variable beam geometries: TXRF, GI-XRF and 45°/45°
- same instrumentation have been used for both XRF and GI-XRF geometry
- energy-dispersive SDD with calibrated response behavior and efficiency

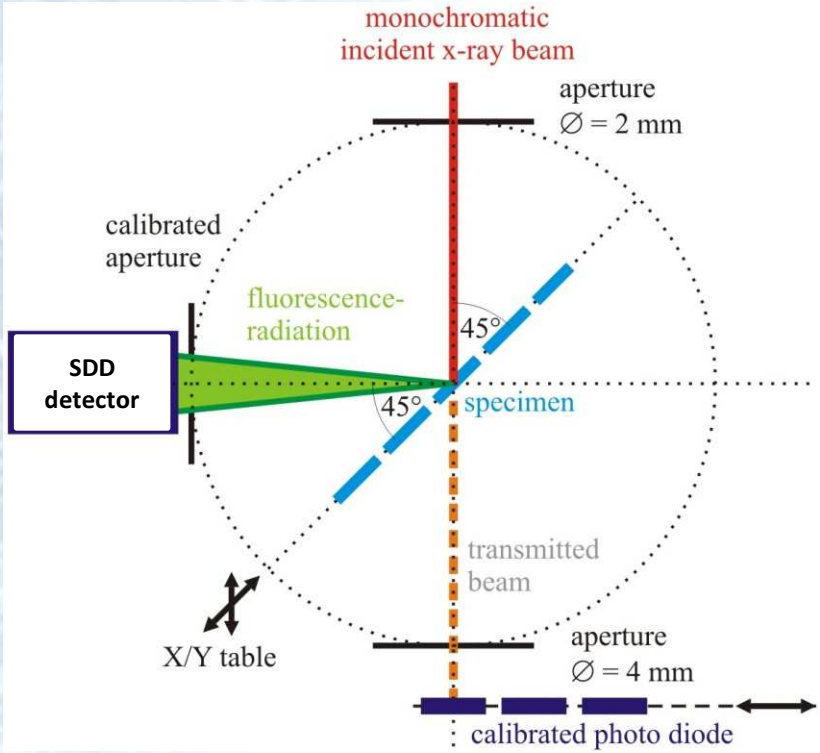

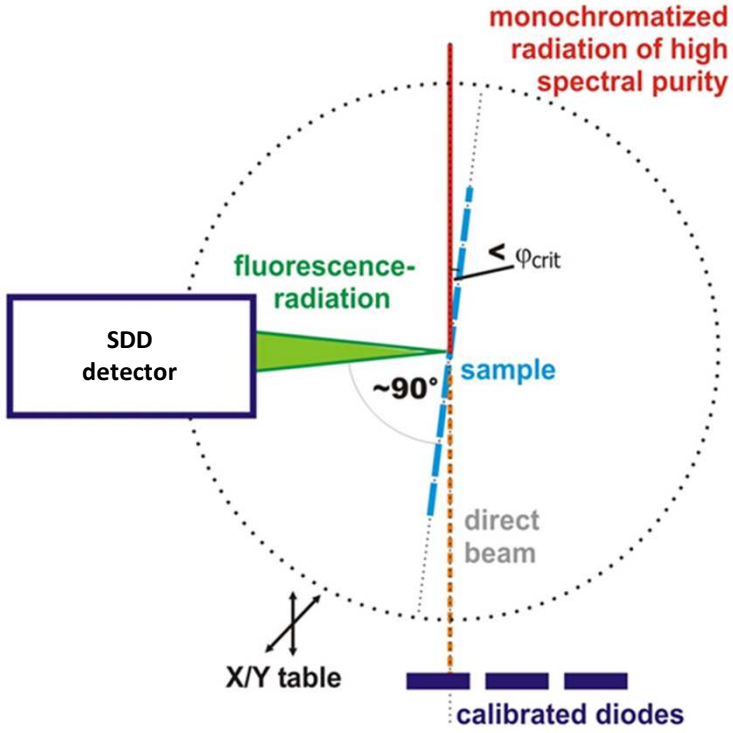

Anal. Chem. 83, 8623-8 (2011)

Results conventional XRF

- example: fluorescence spectrum of the sample without metal layer

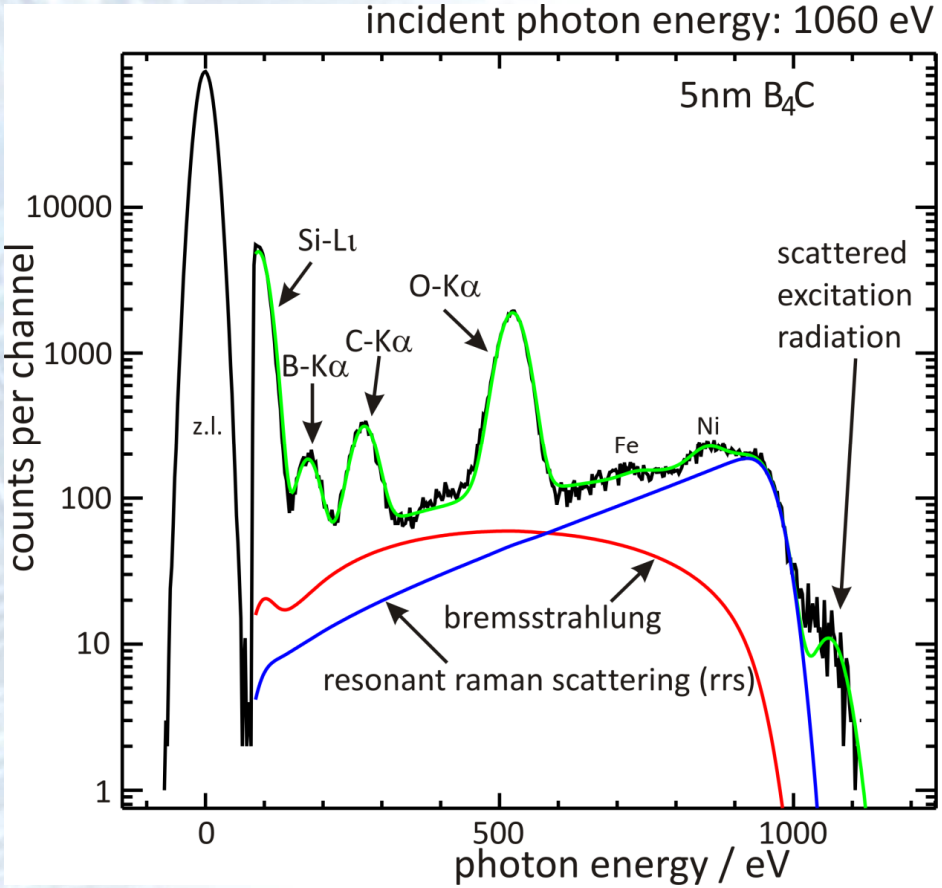

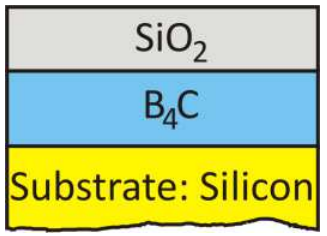

2.5 nm
5 nm

Results conventional XRF

- with Ni metal layer, tailing & shelf of Ni-L lines can cause a high background
- measurement at reduced incident x-ray energies (< Ni L edges)

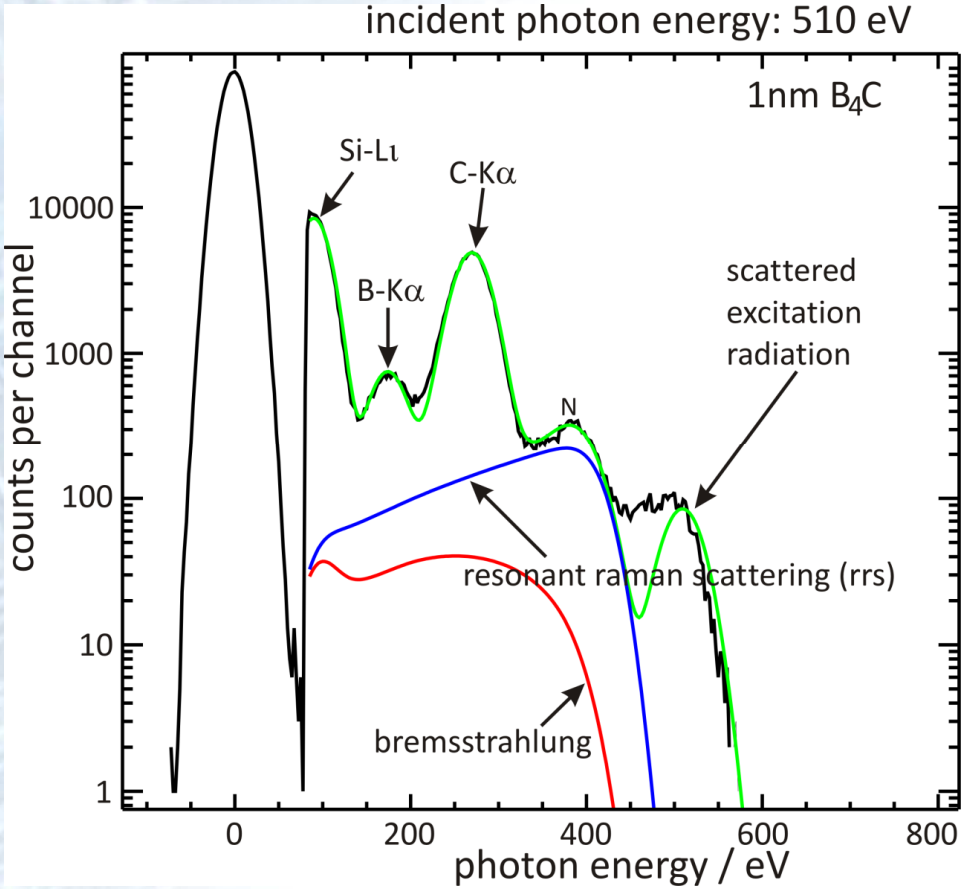

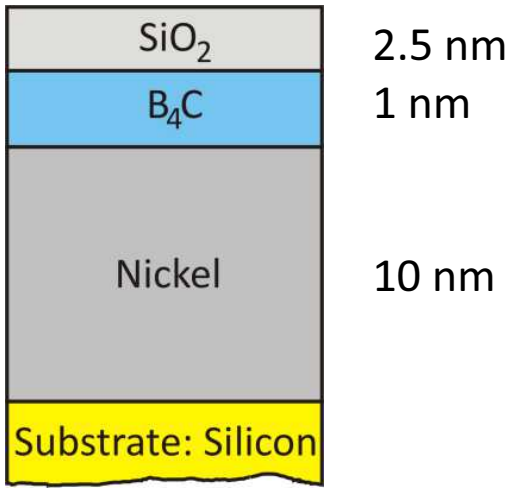

Results grazing incidence XRF

- sample without metal layer
- very shallow incident angle -> only signals of top layer and contaminations
- carbon could be identified as a surface contamination

angular slope of C and B signal

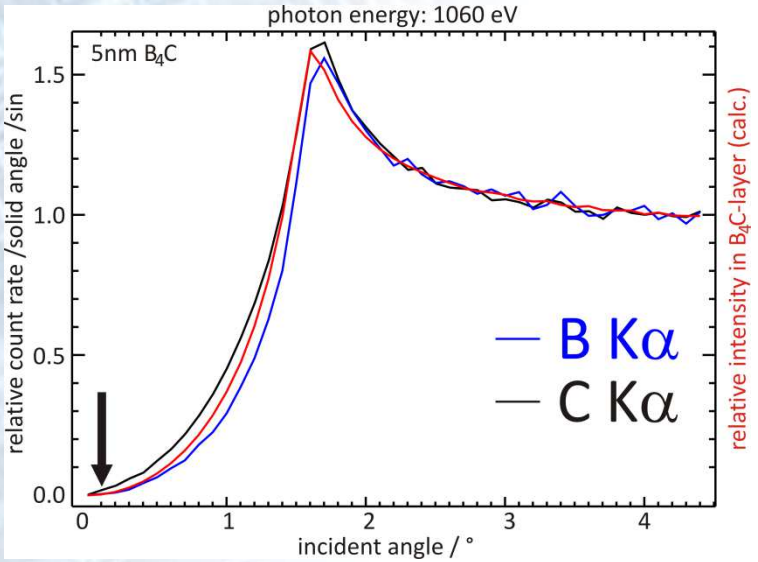

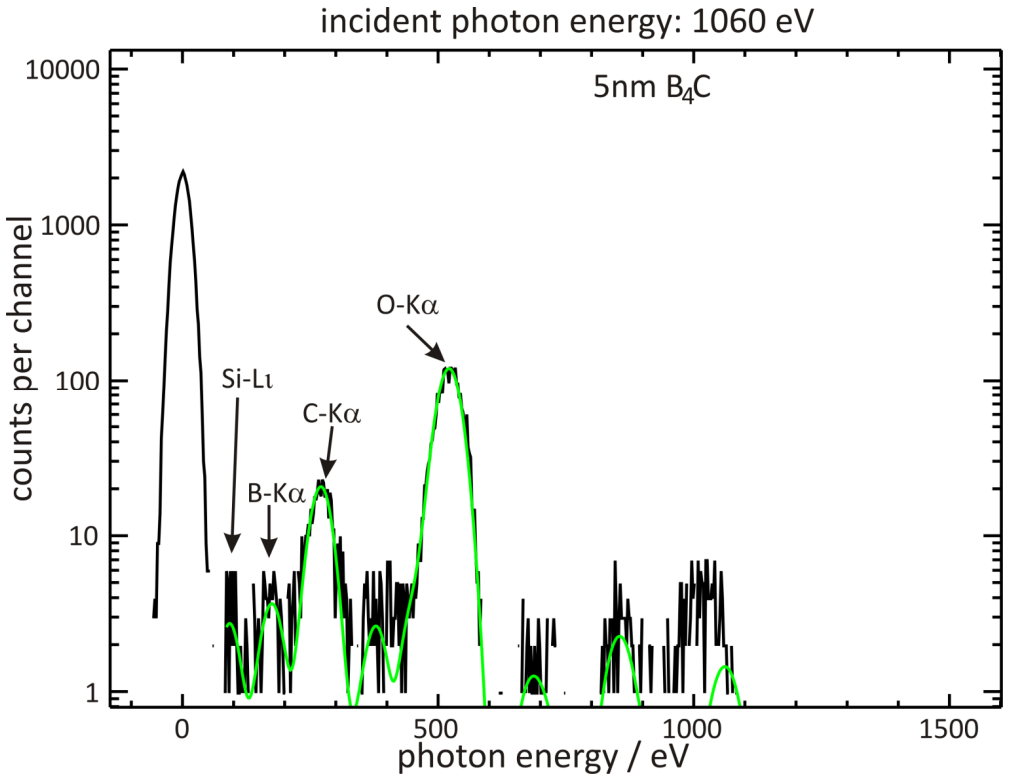

Results grazing incidence XRF

- sample without metal layer
- TXRF angle (70 % of the critical angle of total reflection)
- optimal signal to noise ratio

angular slope of C and B signal

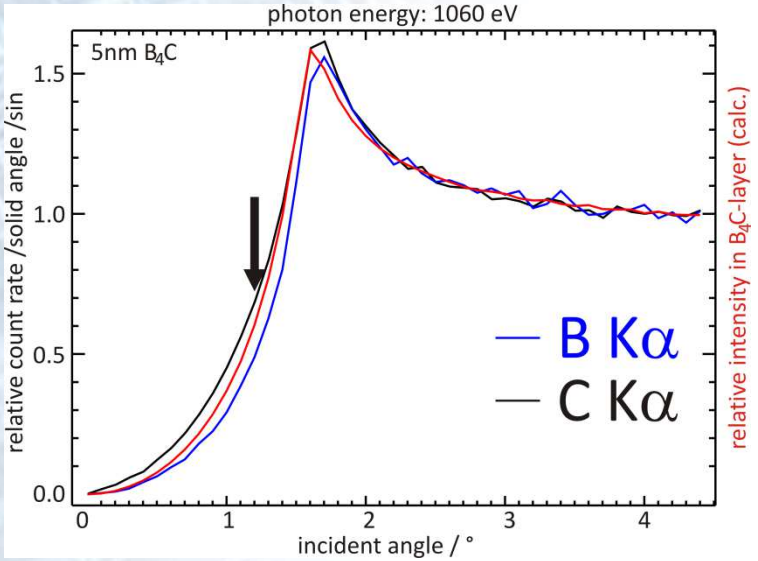

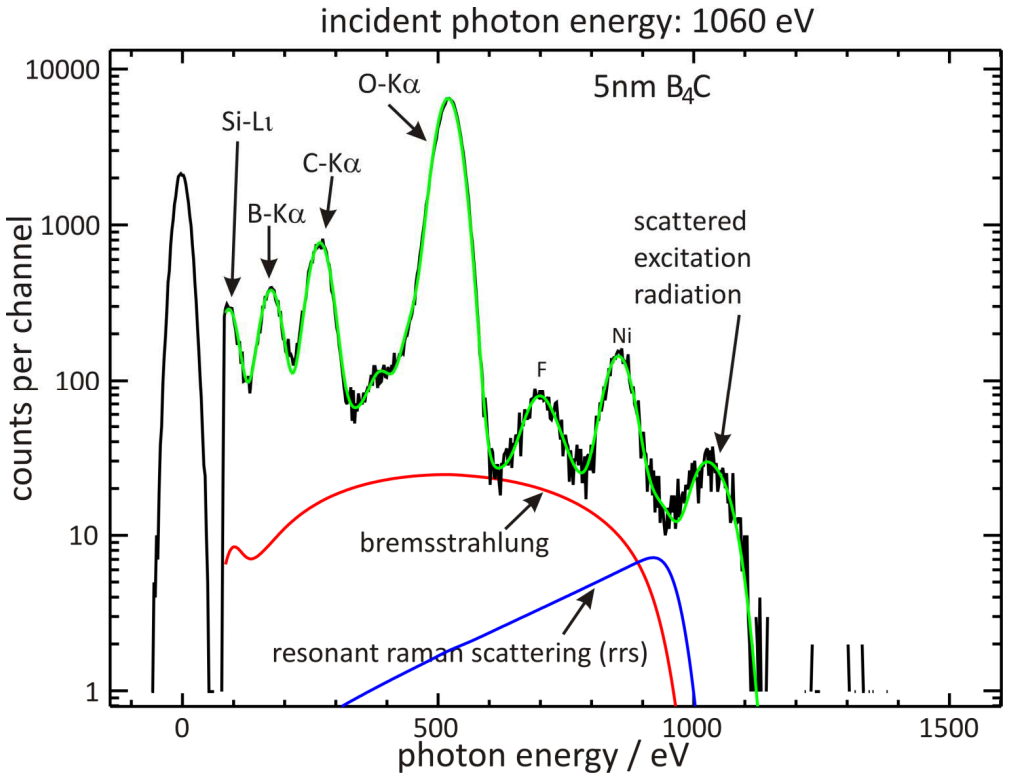

Results grazing incidence XRF

- incidence angle far above the critical angle of total reflection
- increased background contribution due to RRS, bremsstrahlung and scattering
- advantage: low influence of the XSW

angular slope of C and B signal

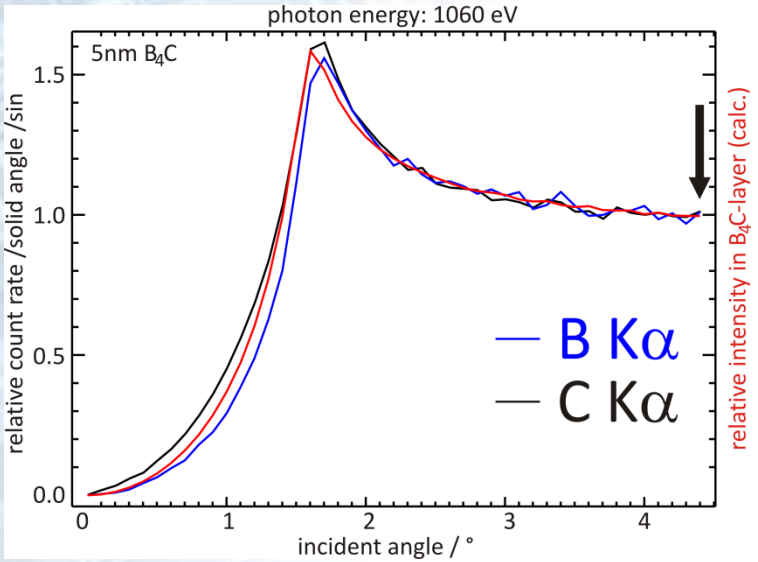

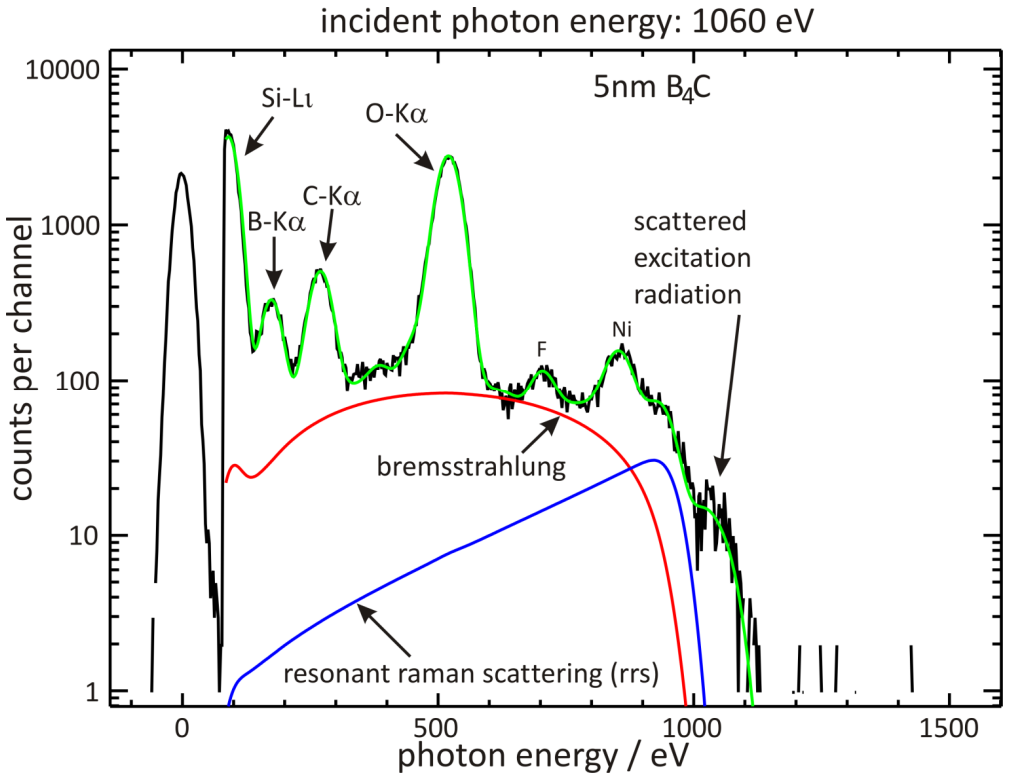

XRF and GI-XRF results (at 510 eV)

- good agreement between XRF and GI-XRF quantification
- increased relative uncertainties for GI-XRF due to XSW calculation and solid angle of detection
- basically high relative uncertainties are caused by the fundamental parameters

reference-free Quantification		1 nm B_4C (0.8 nm B) *nominal*	3 nm B_4C (2.4 nm B) *nominal*	5 nm B_4C (4.0 nm B) *nominal*
without metal layer	XRF	0.9 ± 0.3	2.6 ± 0.7	4.2 ± 1.1
	GI-XRF	0.7 ± 0.3	2.0 ± 1.1	3.8 ± 1.3
with 10nm Ti layer	XRF	0.8 ± 0.3	2.5 ± 0.6	4.0 ± 1.0
	GI-XRF	0.7 ± 0.3	2.3 ± 0.8	3.7 ± 1.2
with 10nm Ni layer	XRF	1.0 ± 0.3	2.7 ± 0.7	4.3 ± 1.1
	GI-XRF	0.6 ± 0.3	1.9 ± 1.0	3.5 ± 1.2

Anal. Chem. 83, 8623-8 (2011)

High-k nanolayers and passivation

PTB

Buried passivation layer on the interface of Ge substrate and high-k nanolayer

- GeOx interface reduces the high-k quality
- preventing oxidation by passivation of Ge surface
- passivation treatment by $(NH_4)_2S$ solution after removal of the native oxide layer (HF-dip)
- potential modification of the passivation by the deposition of 5 nm to 10 nm thick high-k cap layer

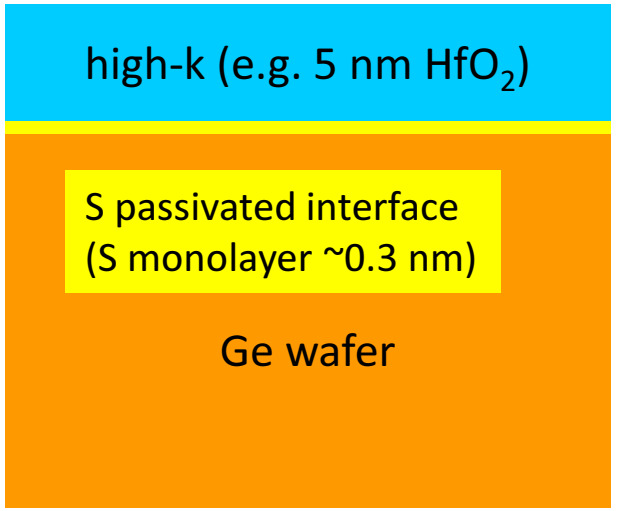

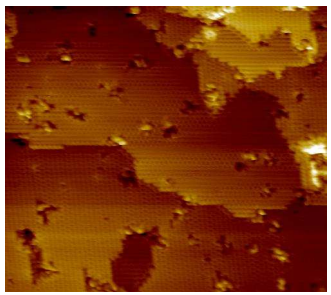

STM image of a passivated Ge surface (50 nm x 50 nm)

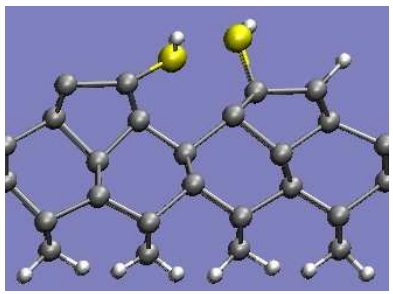

IMEC / K.U. Leuven

Quantification of ALD efficiency

Quantification of Al_2O_3 mass deposition using reference-free XRF in grazing incidence geometry

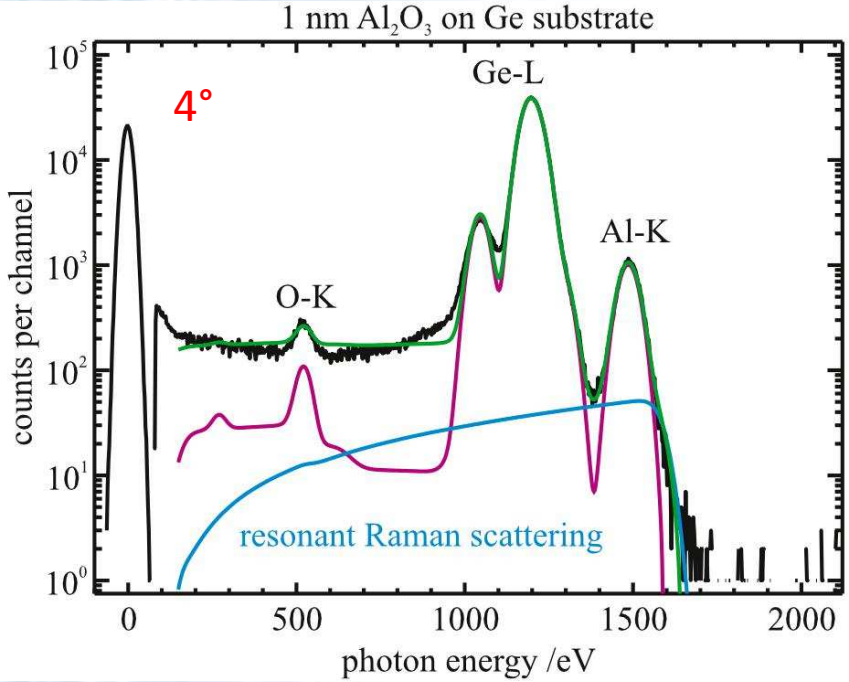

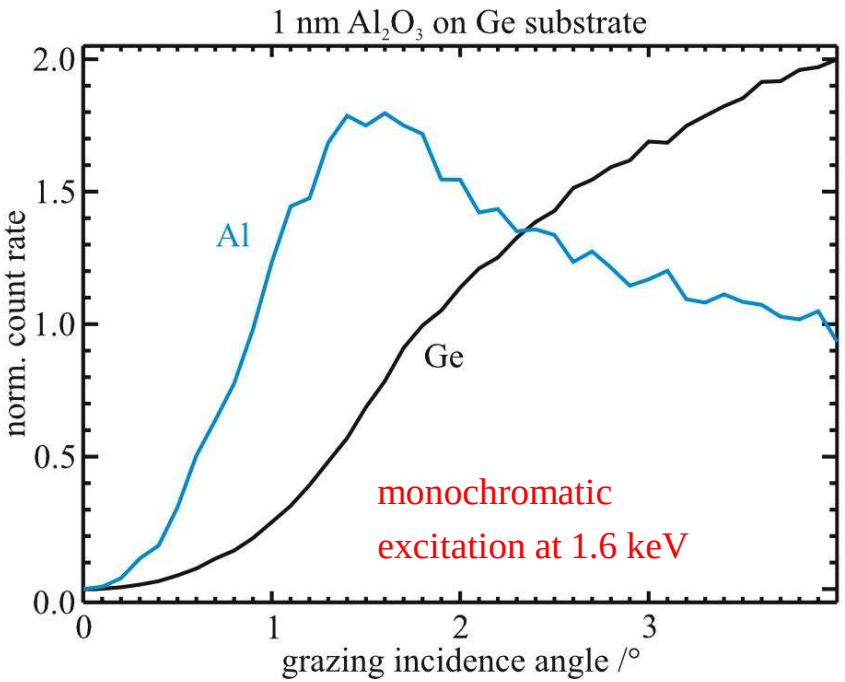

- varying Al_2O_3 layer thickness => changing XSW
- hence measurements performed at 4° incident angle, where no XSW occurs

J. Electrochem. Soc. 158, H1090-H1096 (2011)

Quantification of ALD efficiency

Al_2O_3 on Ge substrate

IMEC & KU Leuven

- How efficient is the ALD deposition of the high-k material?

=> Determination of the mass deposition by GI-XRF

S-passivation	high-k=TMA/H_2O	nm	ng/cm^2
yes	1 cycle	0,05	18
yes	2 cycles	0,06	24
yes	5 cycles	0,13	52
yes	10 cycles	0,33	132
yes	20 cycles	0,86	337
yes	50 cycles	2,5	985

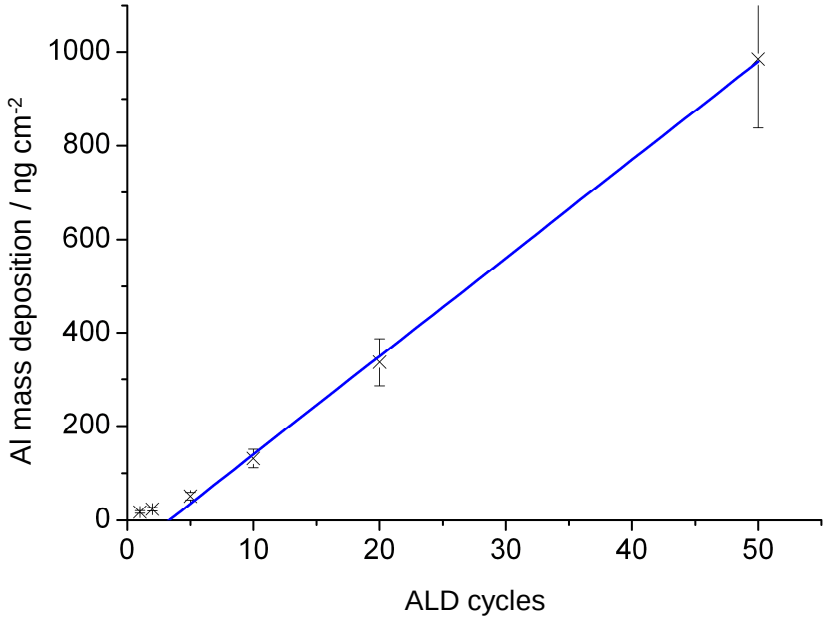

- linear growth on passivated Ge substrate after 2 cycles

J. Vac. Sci. Technol. A 30, 01A127-1 (2012)

Quantification of ALD efficiency

Al_2O_3 on InGaAs substrate

IMEC & KU Leuven

- How efficient is the ALD deposition of the high-k material?

=> Determination of the mass deposition by GI-XRF

S-passivation	high-k= TMA/ H_2O	nm	ng/cm^2
yes	1 cycle	0,078	30,5
yes	2cycles	0,127	49,8
yes	5cycles	0,238	93,5
yes	10 cycles	0,437	164,6
yes	20 cycles	1,011	396,2
yes	50 cycles	2,062	808,5

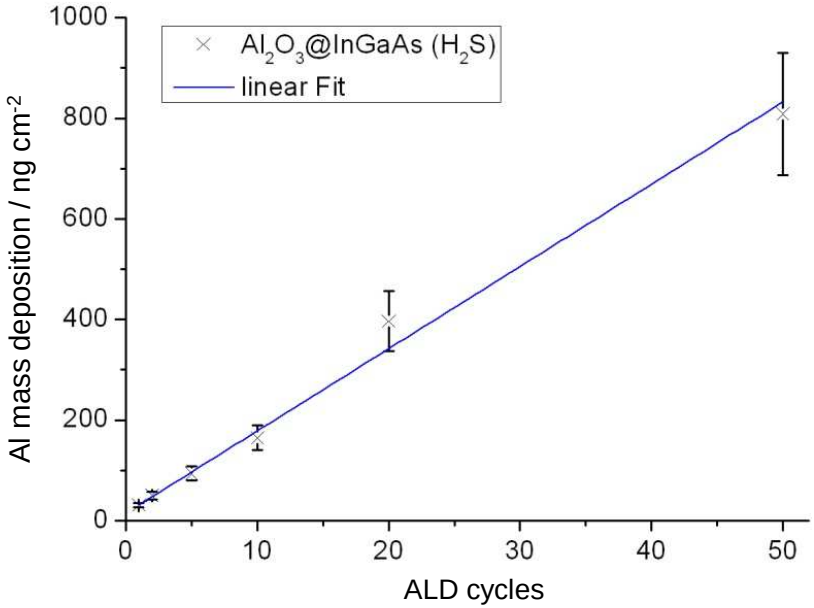

- linear growth on passivated InGaAs substrate after the 1st cycle

J. Vac. Sci. Technol. A 30, 01A127-1 (2012)

Quantification of ALD efficiency

Al_2O_3 on InP substrate

IMEC & KU Leuven

- How efficient is the ALD deposition of the high-k material?
- What is the impact of the passivation layer on the ALD process?

S-passivation	high-k= TMA/H_2O	ng/cm^2
yes	1 cycle	10,2
yes	2 cycles	18,4
yes	3 cycles	26,7
yes	5 cycles	44,5
yes	10 cycles	134,0
yes	20 cycles	322,6
no	1 cycles	8,0
no	2 cycles	13,7
no	3 cycles	18,8
no	5 cycles	36,6
no	10 cycles	106,6
no	20 cycles	311,6

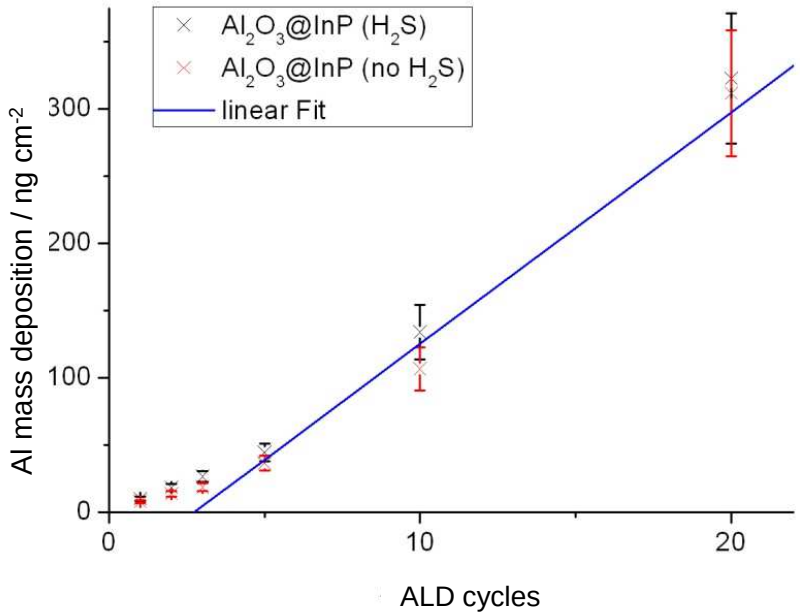

- linear growth on passivated InP after 3 cycles
- impact of passivation is low

Characterization of buried passivation layer

Al_2O_3 on InP substrate

- What happens with the passivation layer during the high-k deposition?

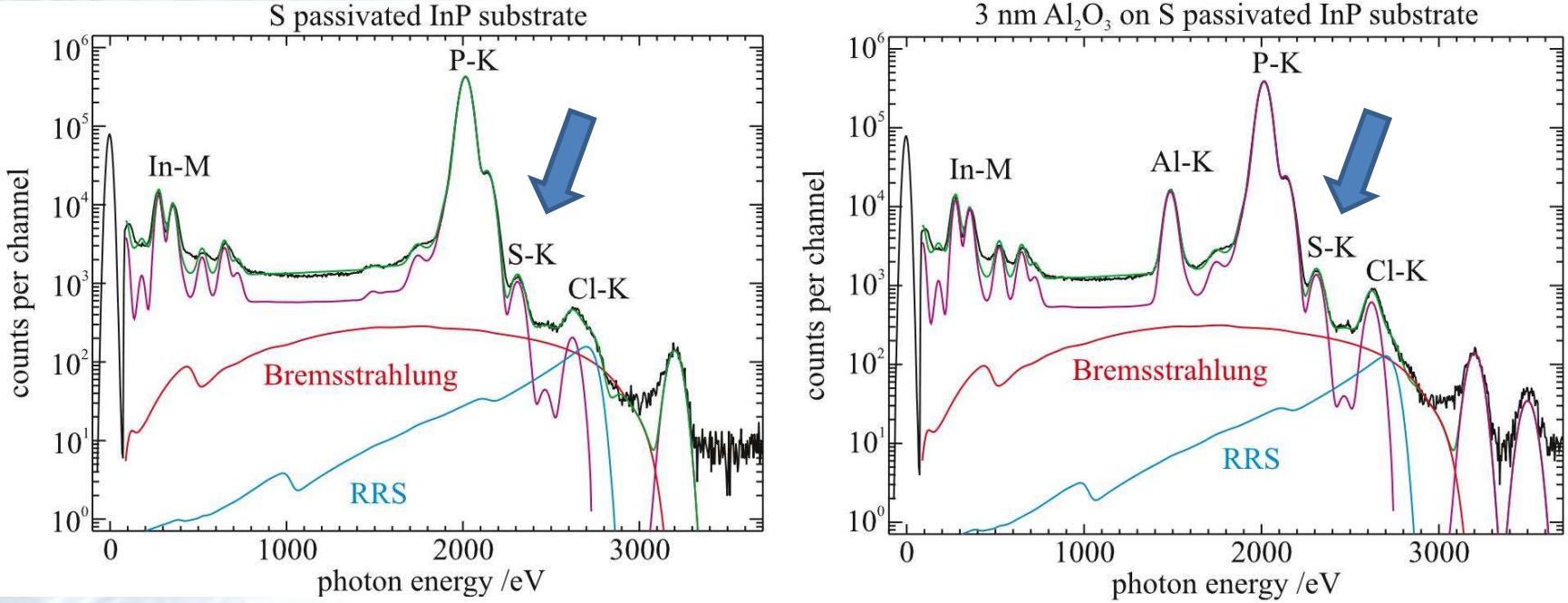

- quantification of sulfur feasible for sub-monolayers

angle of incidence 1.3° ; monochromatic excitation at 3.2 keV

Characterization of buried passivation layer

Al_2O_3 on InP Substrate

- What happens with the passivation layer during the high-k deposition?

=> XRF quantification of the S mass deposition

Al [at/cm²]	Al_2O_3 [nm]	S [at/cm²]
$5.7\ 10^{13}$	0.007	$3.6\ 10^{14}$
$1.8\ 10^{16}$	2.1	$4.9\ 10^{14}$

- sulfur layer is stable at the interface during high-k deposition

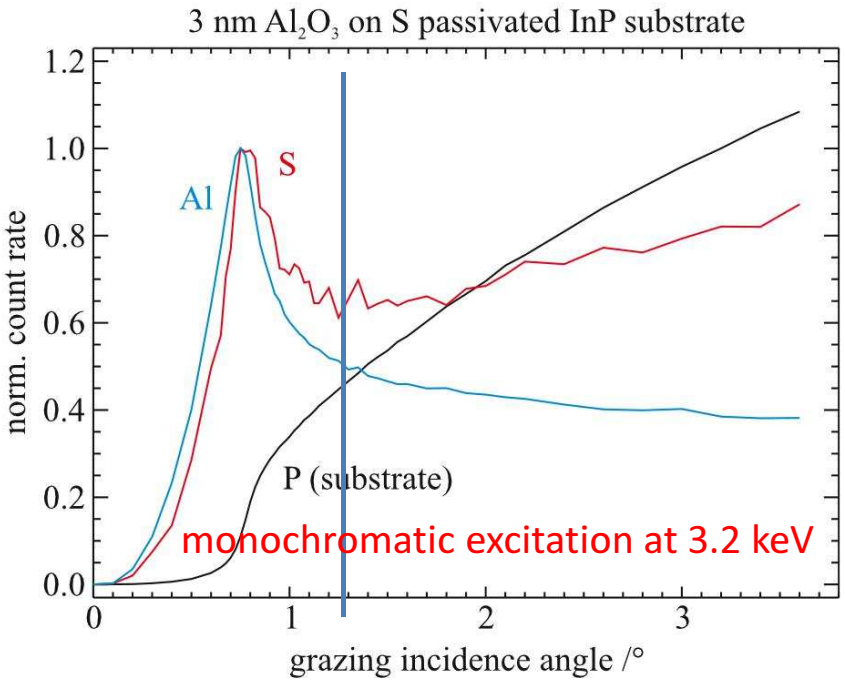

Solid State Phenom. 195, p95 (2013)

Near Edge X-ray Absorption Fine Structure (NEXAFS)

π* resonances occur for unsaturated bonds (=,≡)

π* resonances have lower energies and smaller energetic width than the σ* resonances

resonance energies increase with the bond strength:

$E_{\sigma^*}(\equiv) > E_{\sigma^*}(=) > E_{\sigma^*}(-)$

$E_{\pi^*}(\equiv) > E_{\pi^*}(=)$

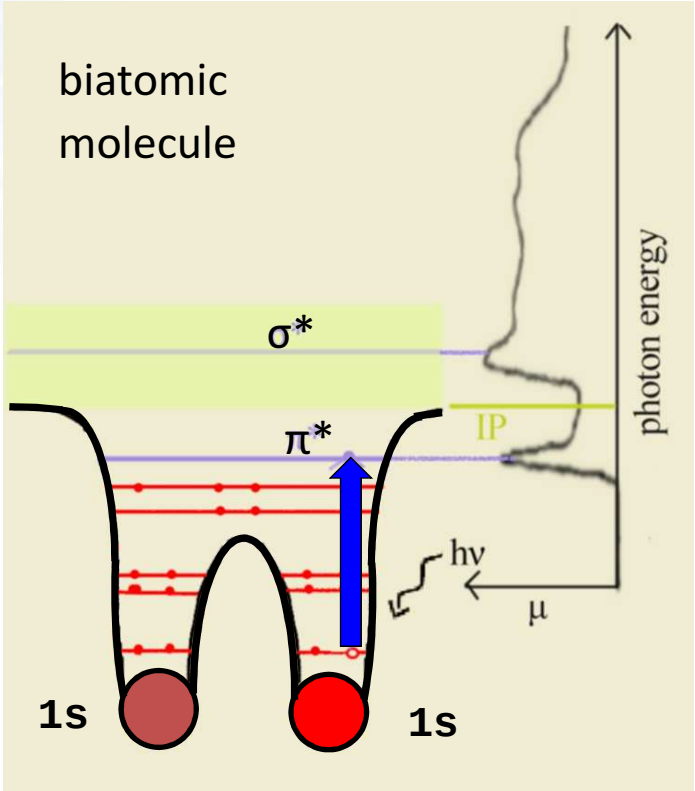

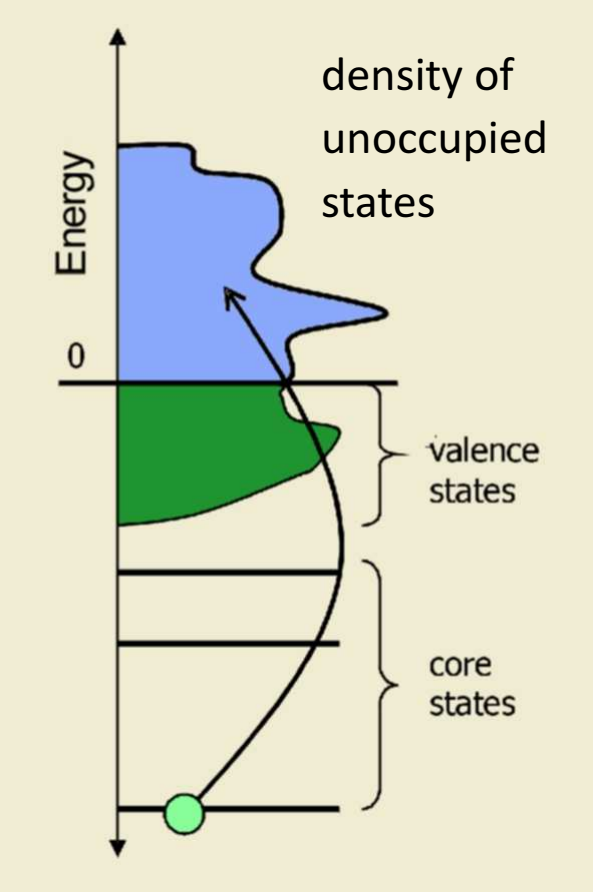

M. Katsikini & E. C. Paloura, Aristotle University of Thessaloniki

Chemical Speciation at the Interface

HfO_2 and Al_2O_3 on Ge substrate

IMEC & KU Leuven

- What happens with the passivation layer during the high-k deposition?

=> Probing the binding state of sulfur at the buried interface

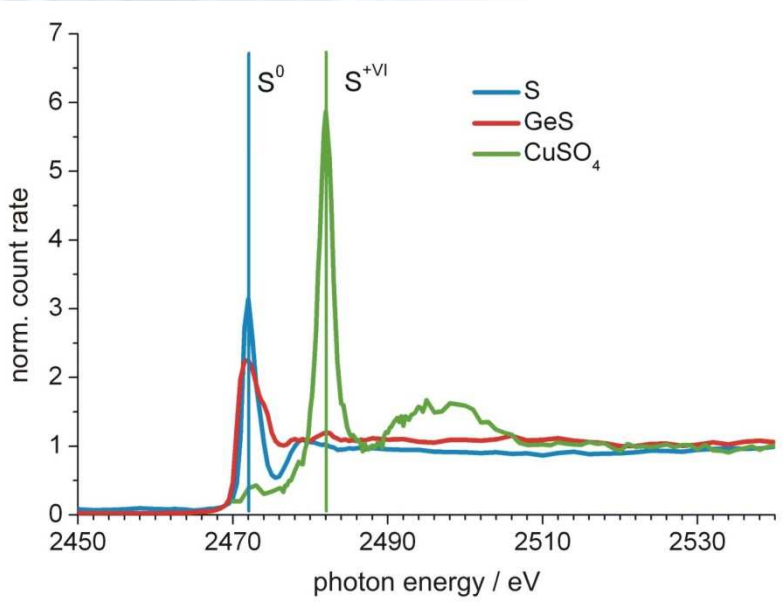

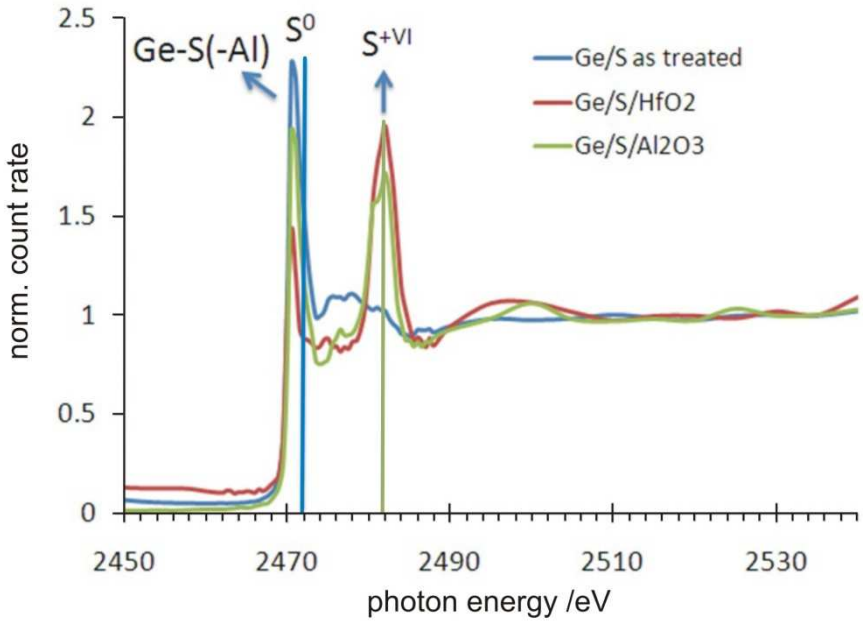

- oxidized sulfur species were observed after high-k deposition
- theory predicts sulfur bonds to the oxygen of the high-k metal oxides

J. Appl. Phys. 110, 084907 (2011)

Novel cathode material for LiS-Batteries

- High theoretical specific energy density (4-5x Li-ion)
- High capacity of charging and discharging

$$S + 2\,Li^+ + 2\,e^- \longleftrightarrow Li_2S$$

- Low cost and abundant resources of sulfur
- Limitation: Loss of active material due to polysulfide dissolution

$$Li_2S \longrightarrow Li_2S_2 \longrightarrow Li_2S_3 \longrightarrow Li_2S_4 \longrightarrow Li_2S_6 \longrightarrow Li_2S_8 \longrightarrow S_8$$

Approach:

- nano- and micro- porous carbon to trap sulfur inside the small pores and access of the active ions through its very high surface area

Objectives material characterization:

- control of intercalation of sulfur into the porous carbon matrix
- which side reactions take place, can we suppress the polysulfide shuttle

X-ray fluorescence spectrum

Typical spectrum of LiS cathode material

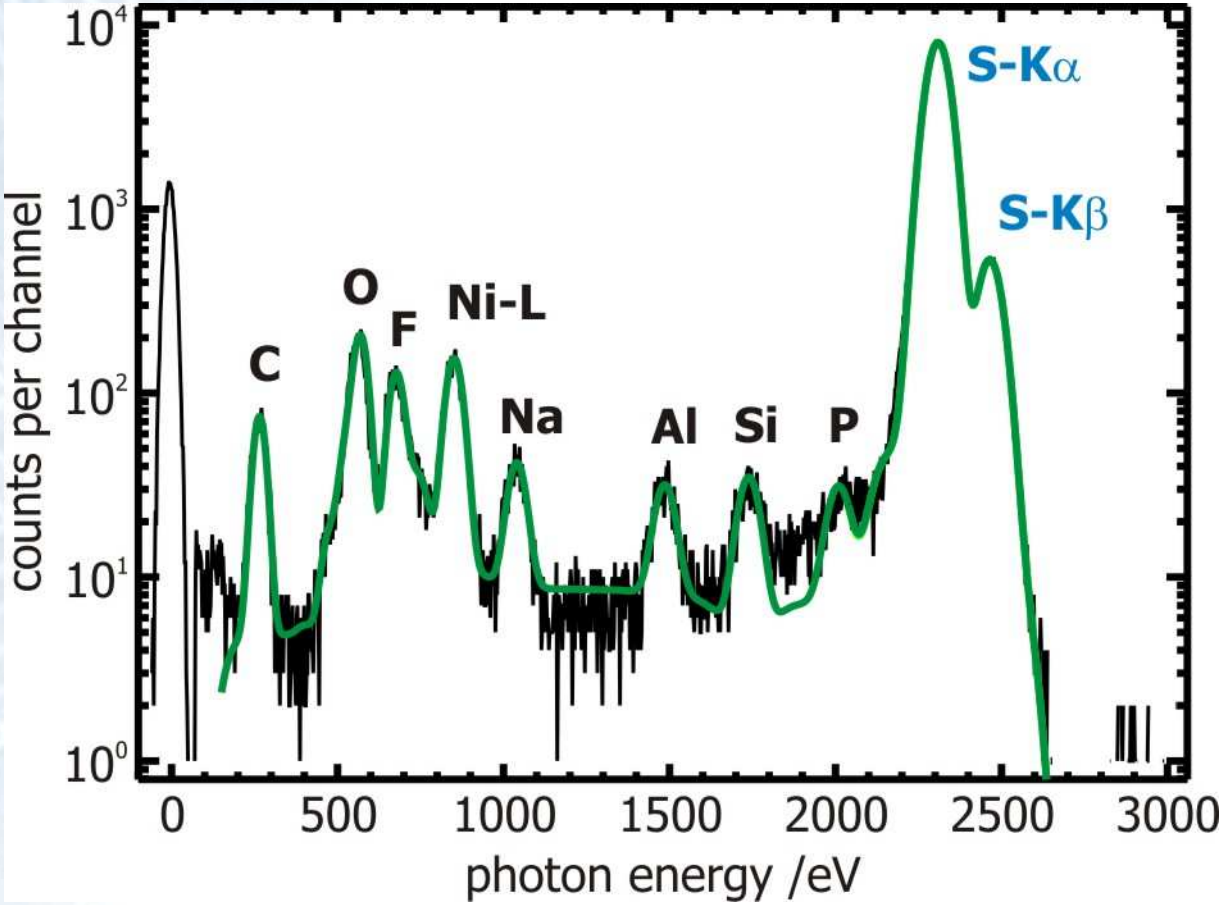

Energy of the incident radiation 2520 eV

Initial LiS cathode material

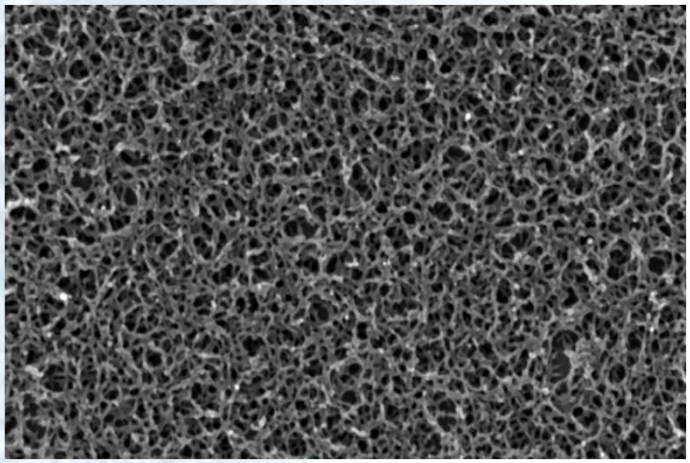

BCP nanotemplate after carbonization

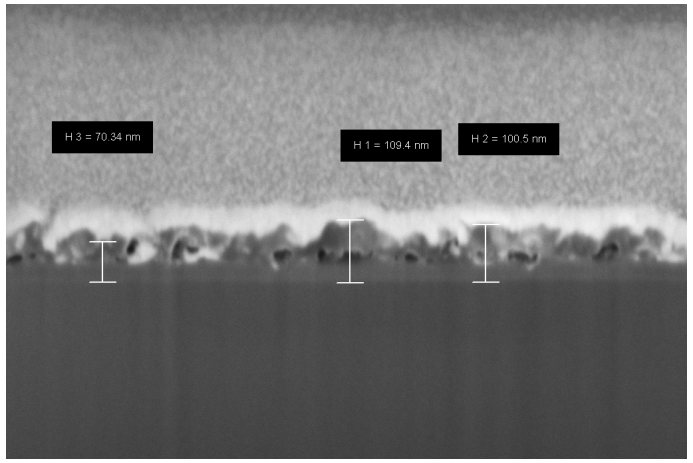

FIB cross section of porous carbon

- Thickness of about 100 nm
- Analytical Questions:
  - Degree of filling with sulfur
  - Depth distribution of sulfur
  - Chemical state of sulfur after intercalation

Initial LiS cathode material

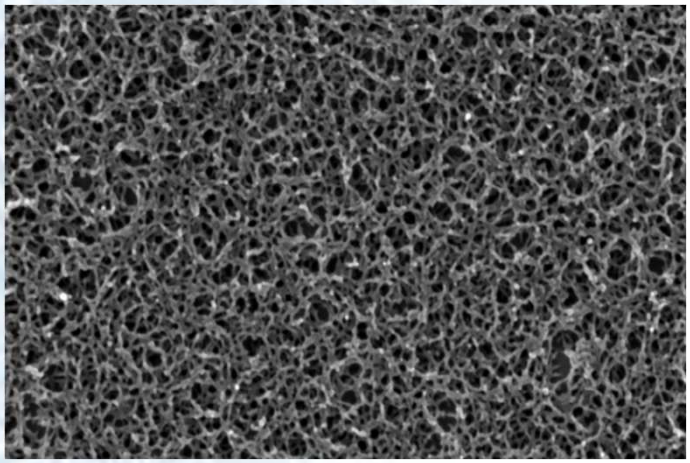

BCP nanotemplate after carbonization

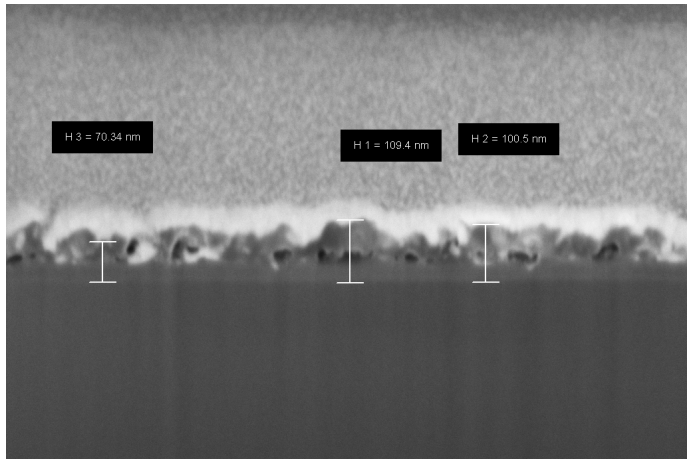

FIB cross section of porous carbon

- GI-XRF profile => indicates that sulfur is homogeneous distributed in depth
- elemental sulfur after intercalation has been confirmed by NEXAFS (melting at 150°)

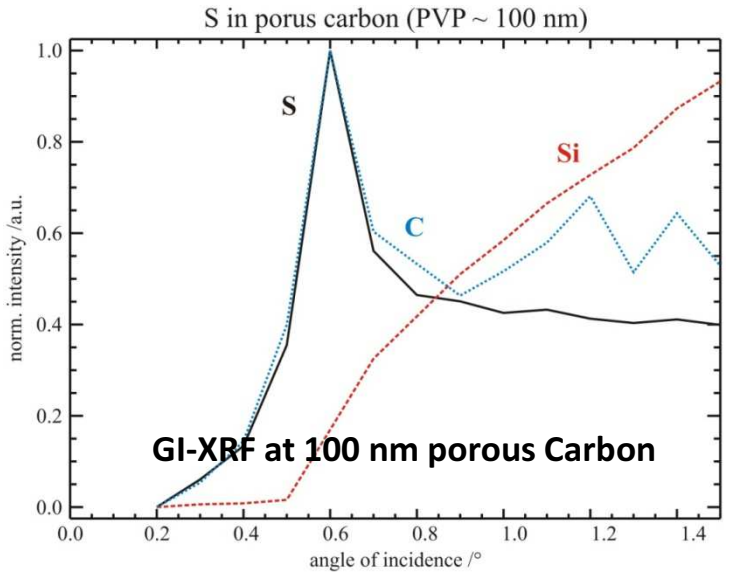

Chemical speciation of thick cathode films

NEXAFS of a porous carbon cathode completely recharged (1 cycle)

- nearly the same structure as for the fresh cathode
- changed ratio of elemental/reduced sulfur to oxidized sulfur

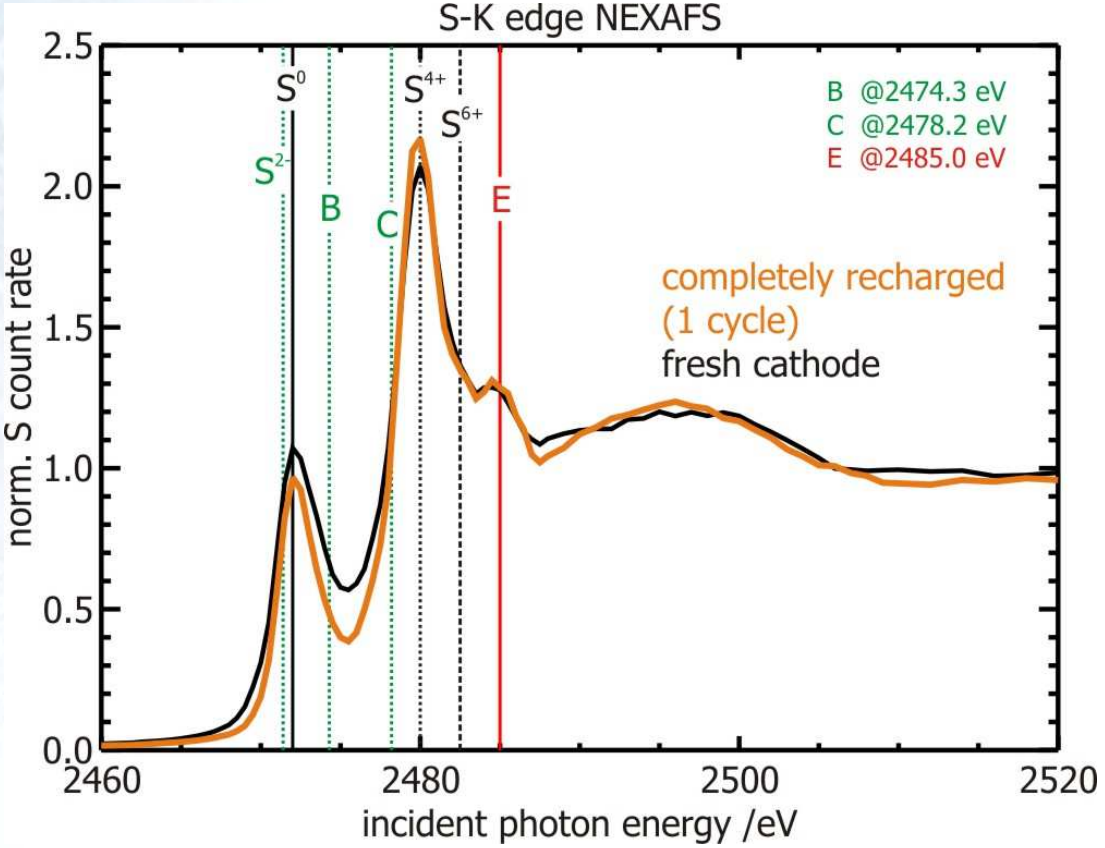

Chemical speciation of thick cathode films

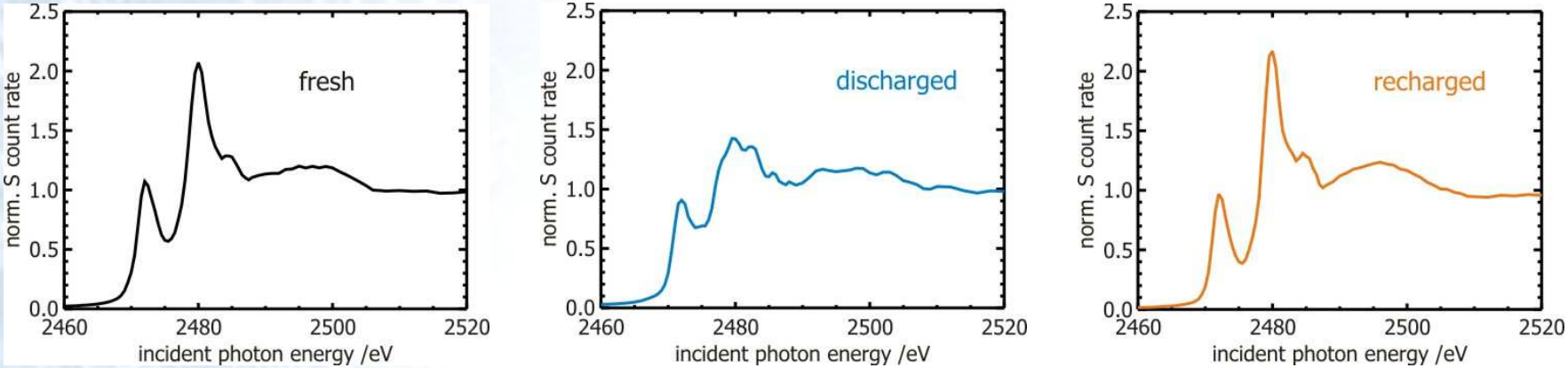

- Discharged cathode shows different NEXAFS structure, similarities with polysulfide
- Recharged cathode shows nearly the same NEXAFS structure as the fresh cathode, but different ratio between S(0) and S(4+) resonance
- Potential problem: oxidation due to ambient air exposure between electrochemical and x-ray spectrometric characterization
- In-situ measurements needed for more reliable correlation

Conclusions and Perspectives

- fundamental parameter based quantification can reduce the dependency to appropriate reference materials
- radiometrically calibrated instrumentation allows for reference-free quantification
- grazing incidence x-ray fluorescence analysis has prove as a powerful tool for non-destructive characterization of nanoscaled materials
- tuning the angle of incidence and the x-ray energy allows to investigate buried interfaces, nanolayers and elemental depth profiles
- combined with x-ray absorption spectroscopy the chemical state can investigated in nanolayered materials
- challenge: in-situ measurements for better correlation of physical and chemical properties with the functionality of the material

Acknowledgement

Thank you for your attention

and for the provision of results:

Sonja Sioncke (IMEC, Belgium)

Claudia Fleischmann (form. KU Leuven, Belgium)

Soumyadip Choudhury (IPF Dresden, Germany)

X-Ray and IR Spectrometry group (PTB, Germany)

and for financial support:

Deutsche Forschungsgemeinschaft

www.ANNA-i3.org